Wavelet Analysis of CHAMP Flux Gate Magnetometer Data

Georgios Balasis, Stefan Maus, Hermann Lühr and Martin Rother

GeoForschungsZentrum Potsdam, Section 2.3, Potsdam, Germany
gbalasis@gfz-potsdam.de

Summary. Wavelet spectral analysis permits quantitative monitoring of the signal evolution by decomposing a time-series into a linear superposition of predefined mathematical waveforms, each with finite duration and narrow frequency content. Thus, the frequency range of the analyzing wavelets corresponds to the spectral content of time-series components. We present a wavelet analysis of 3 years of vector magnetic data from the CHAMP satellite mission. We have detected, identified and classified not only artificial noise sources (e.g. instrument problems and preprocessing errors) but also high frequency natural signals of external fields (e.g. F-region instabilities and pulsations). The results of this analysis will be used for: (a) consequent correction and flagging of the data, (b) derivation of a clean (undisturbed) dataset suitable for the purposes of crustal and main field modeling, and, (c) study of natural signals (e.g. F-region instabilities, pulsations) contained in the data.

Key words: Wavelets, CHAMP FGM Data, Noise, F-region instabilities, Pulsations

1 Introduction

Wavelet transforms began to be used in geophysics in the early 1980s for the analysis of seismic signals. In geophysics the power of wavelets for analysis of nonstationary processes that contain multiscale features, detection of singularities, analysis of transient phenomena, fractal and multifractal processes and signal compression is nowadays being exploited for the study of several mechanisms [1]. Wavelet analysis is becoming a common tool for analyzing localized variations of power within a time-series. By decomposing a time-series into time-frequency space, one is able to determine both the dominant modes of variability and how those modes vary in time [4]. Unfortunately, many studies using time-frequency analysis have suffered from an apparent lack of quantitative results. The wavelet transform has been regarded by many as an interesting diversion that produces colorful pictures, yet purely qualitative results. This misconception is in some sense the fault of wavelet analysis itself, as it involves a transform from a one-dimensional time-series to a diffuse two-dimensional time-frequency image.

The advantage of analyzing a signal with wavelets as the analyzing kernels, is that it enables one to study features of the signal locally with a detail

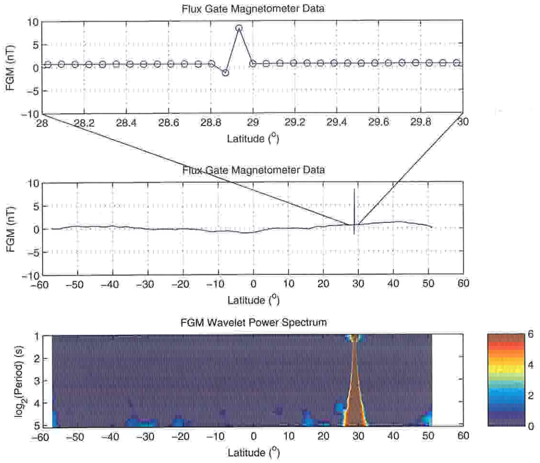

Fig. 1. Orbit with pre-processing error (2 s pulse): variation of the total vector magnetic field with latitude and the associated fingerprint in the wavelet power spectrum. The top diagram zooms in on the 2 s feature. (In all figures the power of the spectrum is given in a log_2 scale.)

matched to their scale. Owing to its unique time-frequency localization [1], wavelet analysis is especially useful for signals that are non-stationary, have short-lived transient components, have features at different scales, or have singularities. The lack of this property makes Fourier transforms inapplicable to the characterization of time-varying signals. Wavelet transforms allow us to identify time-varying frequency content, while Fourier transforms imply a constant frequency content of a time-series.

2 Data and appropriate wavelet basis selection

We performed a time-frequency analysis of the magnetic field magnitude data derived from the CHAMP 1 Hz Flux Gate Magnetometer (FGM) measurements, which were collected from August 2000 to May 2003. From all the CHAMP 1 Hz FGM measurements we selected night time (22:00–06:00 local time, LT), and quiet (Kp<2) orbits. This gave a dataset of ~5000 orbits from which the latitude range from -60° to +60° was considered. The total field was computed from the three vector components. Prior to the analysis, the GFZ main field model POMME-1.4 (*http://www.gfz-potsdam.de/pb2/pb23/index_e.html*) and crustal field model MF2 were subtracted from the data [3].

Wavelet transforms enable us to obtain orthonormal base, as well as non-orthogonal expansions of a signal using time-frequency kernels called "wavelets" that have good properties of localization in time and frequency

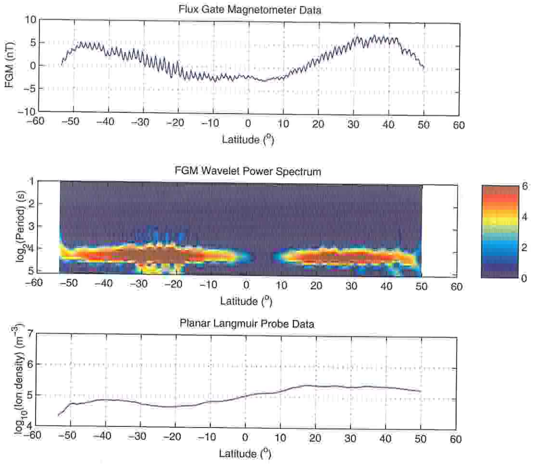

Fig. 2. Orbit with instrument problem (missing torquer correction): variation of the total vector magnetic field with latitude and the corresponding signature in the wavelet power spectrum. The bottom diagram shows that there are no significant variations in the ion density.

domains. The basic idea can be understood as a time-frequency plane that indicates the frequency content of a signal at every time. In any such decomposition the time-frequency plane is layered with cells, called Heisenberg cells, whose minimum area is determined by the uncertainty principle [1]. Heisenberg's uncertainty principle dictates that one cannot measure simultaneously with arbitrarily high resolution in both time and frequency space. The decomposition pattern of the time-frequency plane is predetermined by the choice of the basis function.

In our case, we have used the continuous wavelet transform [4] with the Morlet wavelet as the basis function. Our results were, however, checked for consistency using the Paul and DOG mother functions, as well. Next, we have classified the disturbed segments into orbits: (a) with instrument problems and pre-processing errors, (b) with F-region instabilities, and, (c) with pulsations.

3 Artificial source noise

The wavelet transform can be used to analyze time-series that contain nonstationary power at many different frequencies. For the purposes of our analysis we have focused on the period range between 2 and 32 s. In Fig. 1 we see the fingerpint of an abrupt 2 s pulse in the time-frequency domain. It is depicted as a narrow column of maximum power that dominates all shown frequencies and corresponds to a peak in the time-series at the part of the orbit where

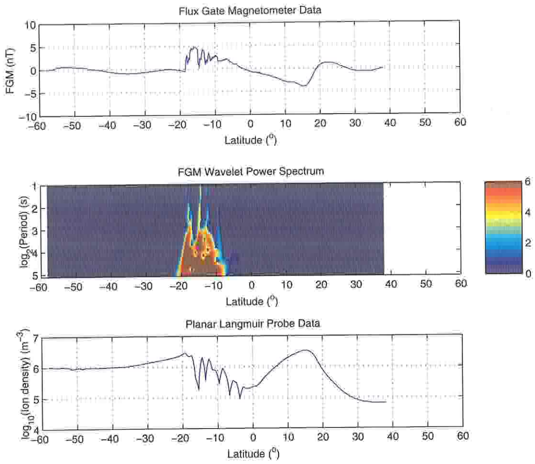

Fig. 3. Orbit with F-region instabilities: total vector magnetic field and its fingerprint in the time-frequency domain. Note that in this and in the following cases the instability is accompanied by a perturbation in the ion density.

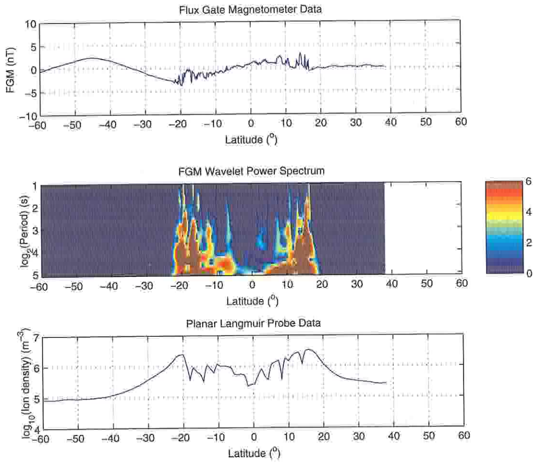

Fig. 4. Orbit with F-region instabilities: this instability region crosses the equator and has an extent of -20° to +20°.

the sudden change occurs in the wavelet power spectrum. The signature of a missing torquer correction looks quite different, from the first case, in the time-frequency space (Fig. 2): it is a zone of maximum power symmetrically located at a 20 s period, almost along the whole orbit. The forms of these two wavelet power spectra directly imply that they cannot be results of physical processes.

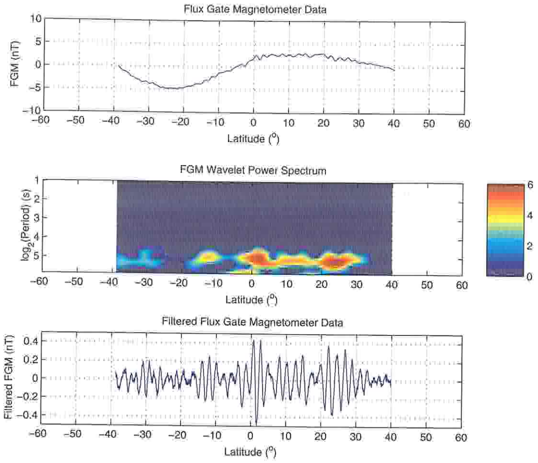

Fig. 5. Orbit with a Pc3 pulsation: total vector magnetic field and its signature in the wavelet power spectrum. The bottom diagram represents the same orbit after applying a 32 s running mean filter.

4 Natural source signals

The CHAMP satellite in its polar, low Earth orbit (below 450 km altitude) is a suitable platform for observing ionospheric instabilities in the F-region [2]. Based on half a year of CHAMP scalar magnetic data it has been suggested that F-region instabilities events are mainly confined in LT to before midnight. Our wavelet analysis of 3 years of vector magnetic data reveals that in principle there is an appreciable occurence rate of F-region instabilities in the LT sector from 22 to 06 (Table 1). These instabilities are generally accompanied by local depletions of the electron density.

In comparison with the artificial signals fingerprints in the time-frequency domain of Sec. 3, we observe physically plausible dispersion in the maximum power regions of the corresponding wavelet power spectra that are signatures of F-region instabilities (Figs. 3–4). These instabilities can be associated with the formation of plasma bubbles [5] that are visible in the Planar Langmuir Probe (PLP) density measurements.

The CHAMP satellite is also capable of monitoring ultra-low-frequency (ULF) magnetospheric waves, called geomagnetic pulsations. In Fig. 5 we observe the wavelet power spectrum of such an event. The form of the maximum power region of this pulsation is somehow similar to the case of the missing torquer correction. However, the frequency that is observed is different (~30 s instead of 20 s for the artificial signal) and the physically expected dispersion is evident in the shape of the highest energy part of the spectrum.

Table 1. Statistics of the examined orbits.

Description	Number of orbits
Total	5078
F-region instabilities	914
Pulsations	105
Pre-processing errors	91
Instrument problems	54

5 Conclusions

We have examined 5078 orbits of FGM (22:00–06:00 LT) data and found 1164 orbits ($\simeq$23%) contaminated by different kinds of artificial (instrument problems, pre-processing errors) and natural sources (F-region instabilities and pulsations) signal. We have managed to derive a clean dataset suitable for users and modellers of the CHAMP vector magnetic data. We have also established a large dataset of $\sim$900 orbits dominated by F-region instabilities. This promissing sample will provide a basis for a better understanding of this external, ionospheric effect, in subsequent work.

Acknowledgement. This work was supported by DFG's research grant MA 2117/3, as part of the Priority Program: "Geomagnetic Variations: Spatio-temporal structure, processes and effects on system Earth", SPP 1097.

References

1. Kumar P, Foufoula-Georgiou E (1997) Wavelet analysis for geophysical applications. Rev Geophys *35*: 385–412.
2. Lühr H, Maus S, Rother M, Cooke D (2002) First in-situ observation of night-time F region currents with the CHAMP satellite. Geophys Res Letters *29*: 127-1–4.
3. Maus S, Rother M, Holme R, Lühr H, Olsen N, Haak V (2002) First scalar magnetic anomaly map from CHAMP satellite data indicates weak lithospheric field. Geophys Res Letters *29*: 47-1–4.
4. Torrence C, Compo GP (1998) A Practical Guide to Wavelet Analysis. Bull Am Meteor Soc *79*: 61–78.
5. Whalen JA (2000) An equatorial bubble: Its evolution observed in relation to bottomside spread F and to the Appleton anomaly. J Geophys Res *105(A3)*: 5303–5315.